Chapter 16. New Developments in Laser Spectroscopy

§16.1 Laser Cooling/Trapping and Ion Trap

Let us consider an atom with rest mass M in the energy level E_i that moves with the velocity v. If this atom absorbs a photon of energy $\hbar\omega_{ik} \simeq E_k - E_i$ and momentum $\hbar k$, it is excited into the level E_k. Its momentum changes from $p_i = M v_i$ before the absorption to

$$p_k = p_i + \hbar k, \tag{14.1}$$

after the absorption (the *recoil effect*, Fig. 14.1).

The relativistic energy conservation demands

$$\hbar\omega_{ik} = \sqrt{p_k^2 c^2 + (M_0 c^2 + E_k)^2} - \sqrt{p_i^2 c^2 + (M_0 c^2 + E_i)^2}. \tag{14.2}$$

When we extract $(M_0 c^2 + E_k)$ from the first root and $(M_0 c^2 + E_i)$ from the second, we obtain by a Taylor expansion the power series for the resonant absorption frequency

1st-order   2nd order   photon recoil

$$\omega_{ik} = \omega_0 + k \cdot v_i - \omega_0 \frac{v_i^2}{2c^2} + \frac{\hbar\omega_0^2}{2Mc^2} + \dots. \tag{14.3}$$

The first term represents the absorption frequency $\omega_0 = (E_k - E_i)$ of an atom at rest if the recoil of the absorbing atom is neglected. The second term describes the linear Doppler shift (first-order Doppler effect) caused by the motion of the atom at the time of absorption. The third term expresses the quadratic Doppler effect (second-order Doppler effect). Note that this term is independent of the direction of the velocity v. It is therefore *not* eliminated by the "Doppler-free" techniques described in Chaps. 7–10, which only overcome the *linear* Doppler effect.
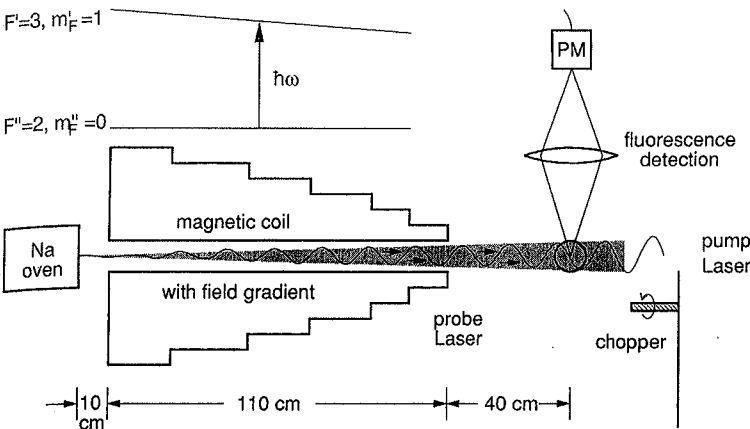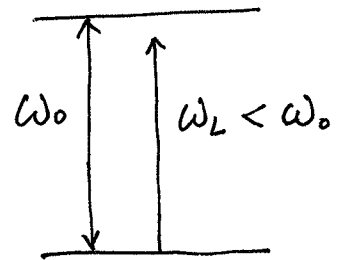
Fig. 14.7. Laser cooling of atoms in a collimated beam with a fixed laser frequency and Zeeman tuning of the atomic absorption frequency [14.19]

To reduce 2nd order Doppler effect (shift and broadening), we must reduce the absolute value of the velocity v.

From energy point of view, absorbed $\hbar\omega_L < \hbar\omega_0$, spontaneous emission $\hbar\omega_0$
∴ Negative net gain of energy → cooling

$$\frac{3}{2} k_B T = \frac{1}{2} m v^2$$

From momentum point of view, $\hbar\vec{k}$ is opposite to atomic momentum

$$\vec{P} = m\vec{v}$$

∴ Momentum is reduced by absorbing opposite direction photon → cooling.
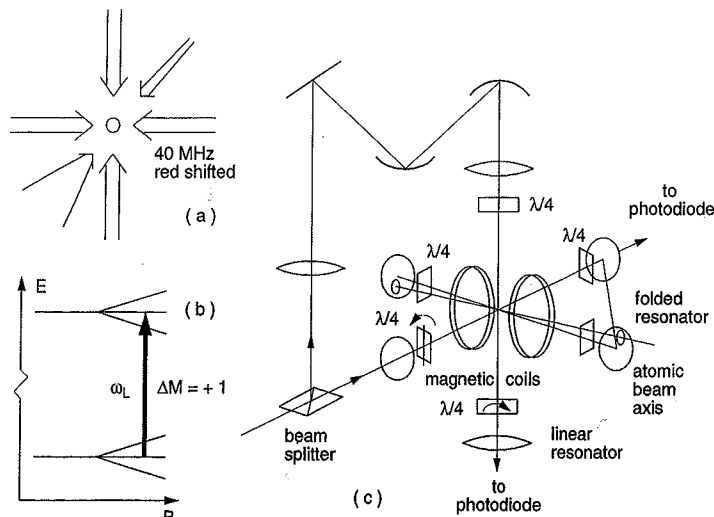
Optical Molasses → Optical Trapping

Fig. 14.18a–c. Realization of optical molasses [14.50a]: (a) laser beam arrangement; (b) Zeeman detuning of the $\Delta M = +1$ transition; and (c) schematic experimental setup

3-D cooling of atoms → optical molasses

All 6 beams are generated by splitting a single laser beam. The laser freq is tuned to the red side of the atomic resonance ($\Delta\omega < 0$), so a repulsive force is always acting on the atoms, which damps the atom velocities.

The effectiveness of the optical molasses for cooling atoms anticipates that the atoms are trapped within the overlap region of the six laser beams for a sufficiently long time. This demands that the potential energy of the atoms shows a sufficiently deep minimum at the center of the trapping volume, i.e., a restoring forces must be present that will bring escaping atom back to the center of the trapping volume. Magneto-Optical Trap (quadrupole) is a very elegant experimental realization of cooling and trapping of atoms: a combination of optical molasses with an inhomogeneous magnetic quadrupole field.
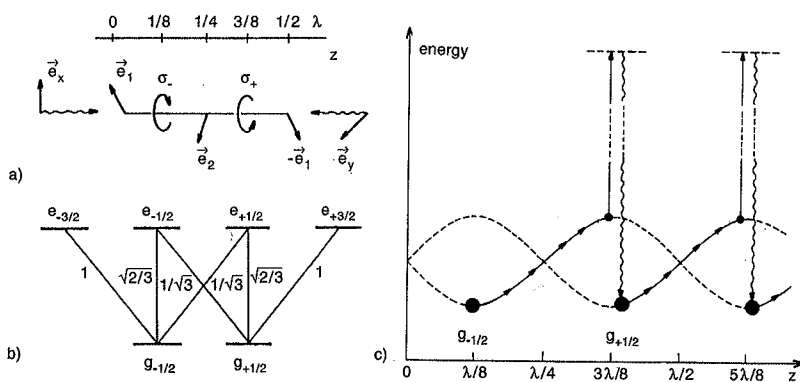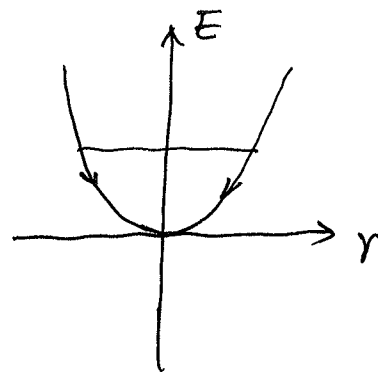

Fig. 14.19a–c. Schematic diagram of polarization gradient (Sisyphus) cooling: (a) two counterpropagating linearly polarized waves with orthogonal polarization create a standing wave with z-dependent polarization. (b) Atomic level scheme and Clebsch–Gordan coefficients for a $J_g = 1/2 \leftrightarrow J_e = 3/2$ transition. (c) Atomic Sisyphus effect in the lin ⊥ lin configuration [14.55]

14.1.9 Bose–Einstein Condensation

At sufficiently low temperatures where the de Broglie wavelength

$$\lambda_{DB} = \frac{h}{m \cdot v} , \qquad (14.38)$$

becomes larger than the mean distance $d = n^{-1/3}$ between the atoms in the cold gas, a phase transition takes place for bosonic particles with integer total spin. More and more particles occupy the lowest possible energy state in the trap potential and are then indistinguishable, which means that all these atoms in the same energy state are described by the same wave function (note that for bosons the Pauli exclusion principle does not apply). Such a situation of a macroscopic state occupied by many indistinguishable particles is called a *Bose–Einstein condensate* (BEC, Nobel prize in physics 2001 for E. Cornell, W. Ketterle, and C. Wiemann).

More detailed calculations show that BEC is reached if

$$n \cdot \lambda_{DB}^3 > 2.612 . \qquad (14.39)$$

With $v^2 = 3k_B T/m$ we obtain the de Broglie wavelength

$$\lambda_{DB} = \frac{h}{\sqrt{3mK_B T}} , \qquad (14.40)$$

and the condition (14.40) for the critical density becomes

$$n > 13.57 (m \cdot k_B T)^{3/2}/h^3 .$$

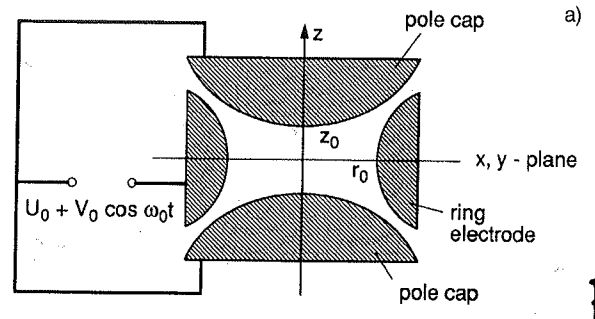The minimum density for BEC depends on the temperature and decreases with $T^{3/2}$ [14.6, 14.59].

Atomic Fountain + Ramsey Fringes

⇓

Cs Atomic Frequency Standard

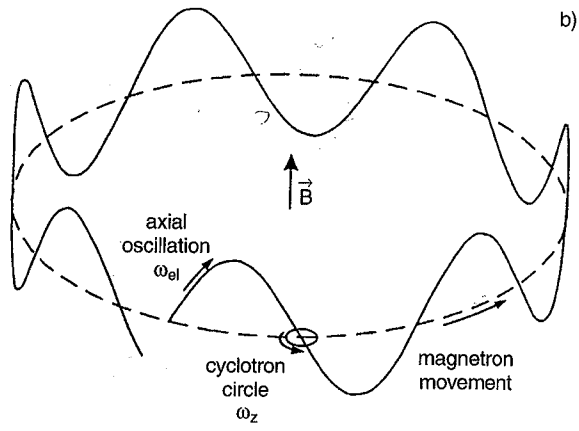9192631770 Hz

Ion Trap: Paul Trap & Penning Trap

Fig. 14.23a,b. Quadrupole RF trap: (a) experimental setup; (b) ion movement

Spectroscopy with single ions that are stored in EM traps and cooled by laser arrangements.

→ Test of fundamental QM and QED

→ Precise frequency standards.

Paul trap — radio frequency quadrupole trap — ions are confined within a hyperbolic electric DC field superimposed by a RF field: zero field at the center for freq. standard.

Penning trap — a DC magnetic field with a superimposed electric field (hyperbolic geometry)

Dehmelt — Nobel Prize in 1989, for development
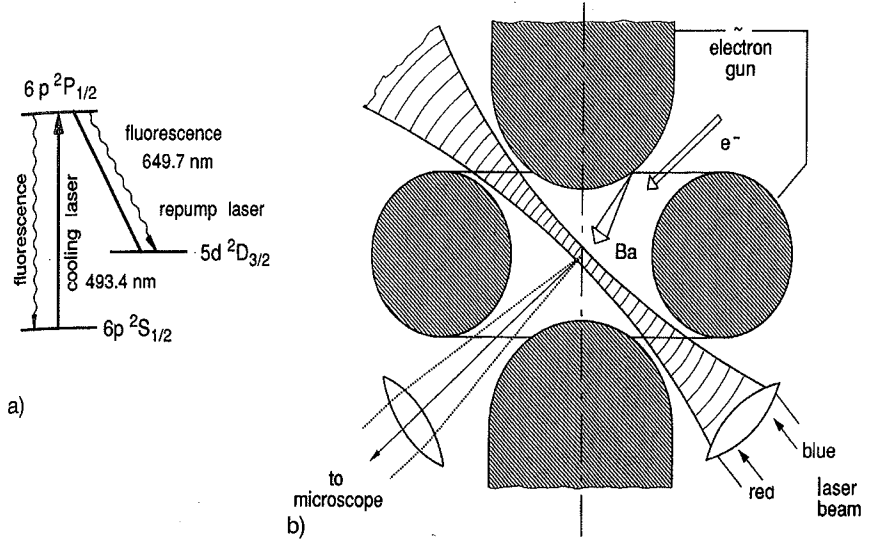Paul — Nobel Prize in 1989 of ion trap,

Fig. 14.25. (a) The Ba$^+$ ion as a three-level system. The second laser at $\lambda = 649.7\,\text{nm}$ pumps the $5d\,^2D_{3/2}$ atoms back into the $6p\,^2P_{1/2}$ level. (b) Experimental arrangement for trapping and cooling of Ba$^+$ ions in a Paul trap [14.77]

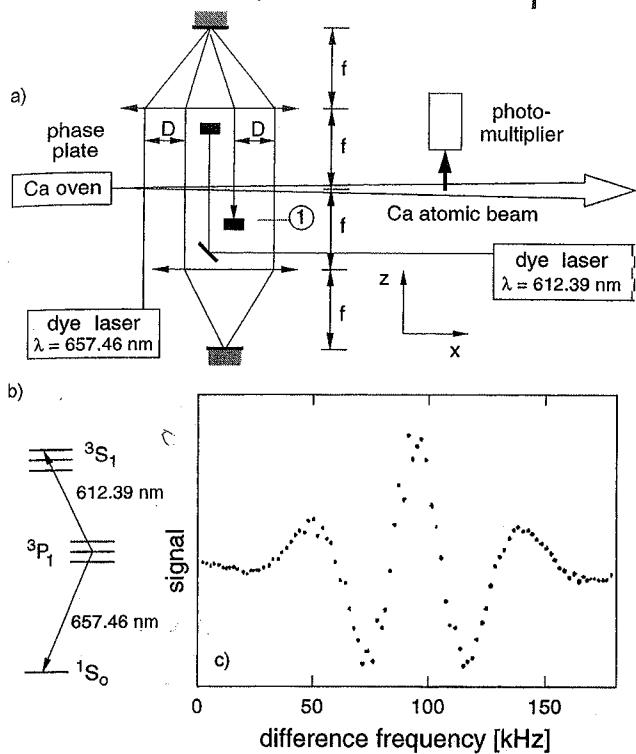# §16.2. Optical Ramsey Fringes and Atom Interferometry

a)

b)

c)

Fig. 14.44a–c. Suppression of one recoil component by optical pumping with a second laser: (a) experimental setup; (b) level scheme; and (c) Ramsey resonance of the remaining recoil component [14.115]

Atom Interferometry

Fig. 14.45. Optical Ramsey scheme of an atomic beam passing through four traveling laser fields, interpreted as matter-wave interferometer. *Solid lines* represent the high-frequency recoil components, *dotted lines* the low-frequency components (only those traces leading to Ramsey resonances in the fourth zone are drawn) [14.122]

Atom Laser

Atoms in a Bose–Einstein condensate are coherent because they are all described by the same wavefunction. If these atoms are released out of the trap (for instance, by a radio-frequency field (Fig. 14.47), or by switching off the magnetic field, which forms the trap potential) the atoms fall under the influence of gravity down as a parallel beam in the $-z$-direction, where all atoms are in the same coherent state. Since this is in analogy to the coherent beam of photons in a laser, this coherent beam of atoms is called an "atom laser." The first realization was a pulsed atom laser, where part of the BEC atoms were released by an RF pulse [14.124]. In addition, quasi-continuous atom lasers have also been realized [14.125]. Using a weak radio frequency field as output coupler with a small coupling strength, atoms could be continuously extracted from the BEC over a period of up to 100 ms. The duration was limited by the finite number of atoms in the BEC. There have been attempts to continuously load the BEC and continuously extract the atoms, which would give a true cw atom laser.
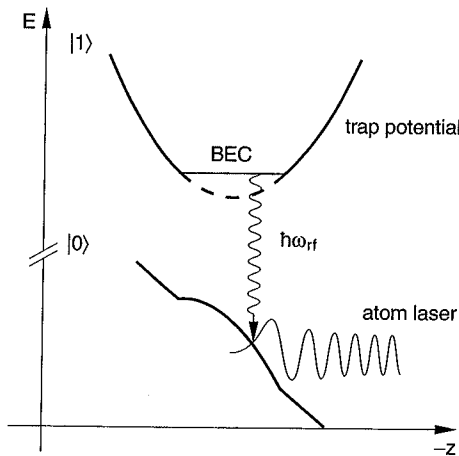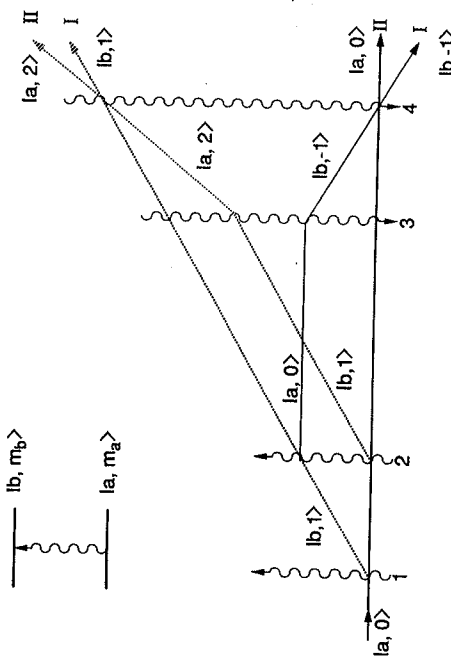
Fig. 14.47. Generation of an atom laser by extracting atoms out of a BEC

14.6 Spectral Resolution Within the Natural Linewidth

Assume that all other line-broadening effects except the natural linewidth have been eliminated by one of the methods discussed in the previous chapters. The question that arises is whether the natural linewidth represents an insurmountable natural limit to spectral resolution. At first, it might seem that Heisenberg's uncertainty relation does not allow outwit the natural linewidth (Sect. 3.1). In order to demonstrate that this is not true, in this section we give some examples of techniques that do allow observation of structures *within* the natural linewidth. It is, however, not obvious that all of these methods may really increase the amount of information about the molecular structure, since the inevitable loss in intensity may outweigh the gain in resolution. We discuss under what conditions spectroscopy within the natural linewidth may be a tool that really helps to improve the quality of spectral information.

Fig. 14.51a,b. Gated detection of exponentional fluorescence decay with a gate function $f(t)$: (a) schematic scheme; (b) experimental realization

With incoherent techniques, no narrowing of the natural linewidth can be achieved, even if only fluorescence photons from selected long-living atoms with $t > T \gg \tau$ are selected.

However, if instead of the intensity, the amplitude or an intensity representing a coherent superposition of amplitude can be measured, where the phase information and its development in time is preserved, then line narrowing can be observed. Such measurements are possible with one of the coherent technique, e.g., Quantum Beat or Level-crossing.

§16.4 Absolute Optical Frequency Measurement

$$\nu_{10} = 520.206\ 837$$

| $\frac{\nu_{10}}{2}$ (He - Ne) 1.15 μm | → | X 2 | → | ν_{10} ($^{127}I_2$) | → |

$\nu_{10} = 2\nu_9 + \nu_{10\,B}$ ⊗

$\nu_9 = 260.103\ 264$ Ne (^{20}Ne)

$\nu_9 = \nu_8 + \nu'_{CO_2} + \nu''_{CO_2} + \nu_{9\,B}$ [SA]⊗←[XTAL]←[XTAL]— $^{13}C^{16}O_2$ 9 μm R(20) / $C^{16}O_2$ 9 μm R(22)

$\nu_8 = 196.780\ 372$ He - Ne (1.52 μm)

$\nu_8 = \nu_7 + \nu_{CO} + \nu_{8\,B}$ [SA]←⊗← $\nu = 48.862\ 064$ CO (6.1 μm)

$\nu_7 = 147.915\ 857$ Xe (2.03 μm)

$\nu_7 = \nu_6 + \nu'_{CO_2} + \nu''_{CO_2} + \nu_{7\,B}$ [SA]←⊗← $\nu_{6,7'}$ CO_2 9 μm P(36) / $\nu_{6,7''}$ CO_2 10 μm P(8)
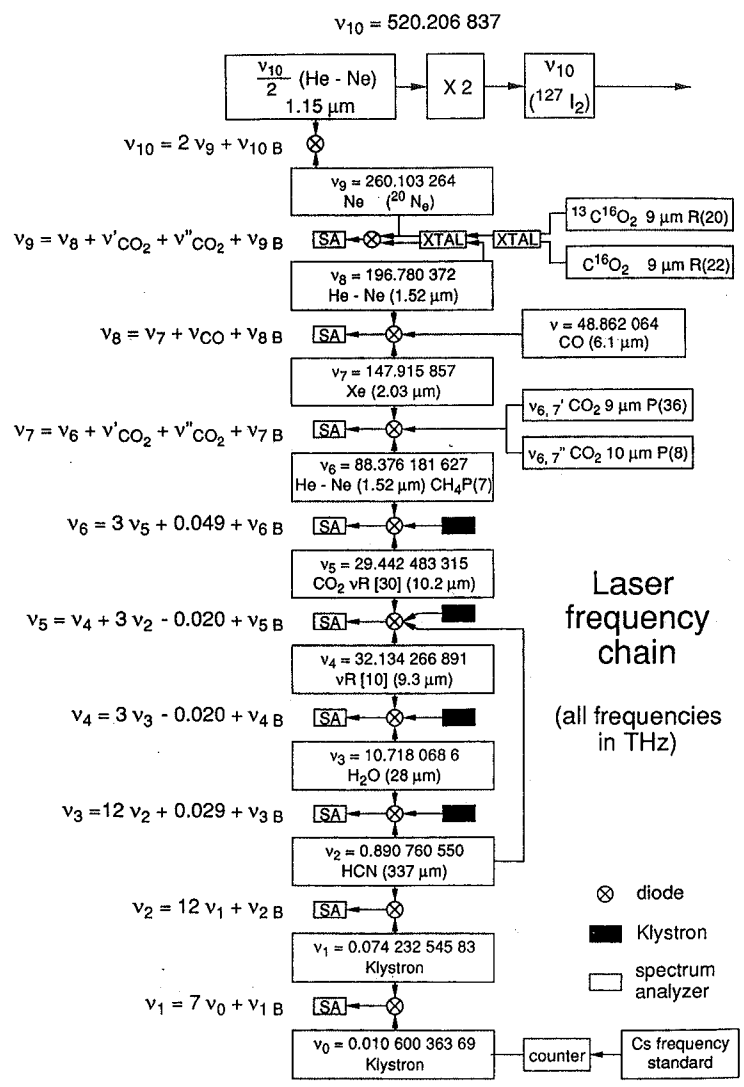
$\nu_6 = 88.376\ 181\ 627$ He - Ne (1.52 μm) CH_4P(7)

$\nu_6 = 3\nu_5 + 0.049 + \nu_{6\,B}$ [SA]←⊗←■

$\nu_5 = 29.442\ 483\ 315$ CO_2 νR [30] (10.2 μm)

Laser frequency chain

(all frequencies in THz)

$\nu_5 = \nu_4 + 3\nu_2 - 0.020 + \nu_{5\,B}$ [SA]←⊗←■

$\nu_4 = 32.134\ 266\ 891$ νR [10] (9.3 μm)

$\nu_4 = 3\nu_3 - 0.020 + \nu_{4\,B}$ [SA]←⊗←■

$\nu_3 = 10.718\ 068\ 6$ H_2O (28 μm)

$\nu_3 = 12\nu_2 + 0.029 + \nu_{3\,B}$ [SA]←⊗←■

$\nu_2 = 0.890\ 760\ 550$ HCN (337 μm)

$\nu_2 = 12\nu_1 + \nu_{2\,B}$ [SA]←⊗

$\nu_1 = 0.074\ 232\ 545\ 83$ Klystron

$\nu_1 = 7\nu_0 + \nu_{1\,B}$ [SA]←⊗

$\nu_0 = 0.010\ 600\ 363\ 69$ Klystron —[counter]←[Cs frequency standard]

⊗ diode
■ Klystron
▭ spectrum analyzer

Fig. 14.58. Optical frequency chain that connects the frequency of stabilized optical lasers with the Cs frequency standard [14.150]

§16.5 Squeezing

For very low light intensities the quantum structure of light becomes evident by statistical fluctuations of the number of detected photons, which lead to corresponding fluctuations of the measured photoelectron rate (Sect. 12.6). This *photon noise*, which is proportional to $\sqrt{N}$ at a measured rate of N photoelectrons per second, imposes a principal detection limit for experiments with low-level light detection [14.158]. Additionally, the frequency stabilization of lasers on the millihertz scale is limited by photon noise of the detector that activates the electronic feedback loop [14.159].

It is therefore desirable to further decrease the photon-noise limit. At first, this seems to be impossible because the limit is of principal nature. However, it has been shown that under certain conditions the photon-noise limit can be overcome without violating general physical laws. We will discuss this in some more detail, partly following the representation given in [14.160, 14.161].